Inorg. Chem. **2004**, *43*, 7127–7140

Mononuclear and Dinuclear Monoperoxovanadium(V) Complexes with a Hetero Ligand. 1.[1] Self-Decomposition Reaction, Detection of Reactive Oxygen Species, and Oxidizing Ability

Kan Kanamori,*,† Kazuya Nishida,† Nanako Miyata,† Toshiyuki Shimoyama,† Kaori Hata,† Chie Mihara,† Ken-ichi Okamoto,‡ Yuriko Abe,§ Shingo Hayakawa,|| and Seiichi Matsugo||

Department of Chemistry, Faculty of Science, Toyama University, Gofuku 3190, Toyama 930-8555, Japan, Department of Chemistry, University of Tsukuba, Tsukuba, Ibaraki 305-8571, Japan, Department of Chemistry, Faculty of Science, Nara Women's University, Kitauoyanishi, Nara 630-8015, Japan, and Division of Biotechnology, Interdisciplinary Graduate School of Medicine and Engineering, University of Yamanashi, Kofu 400-8511, Japan

Received October 6, 2003

A mononuclear peroxovanadium(V) complex with histamine-*N,N*-diacetate (histada), K[$VO(O_2)$(histada)], and a dinuclear peroxovanadium(V) complex with 2-oxo-1,3-diaminopropane-*N,N,N′,N′*-tetraacetate (dpot), $Cs_3[(VO)_2(O_2)_2$-(dpot)], were prepared and characterized. The self-decomposition reaction was examined for these peroxovanadium-(V) complexes as well as for K[$VO(O_2)$(cmhist)] (cmhist = *N*-carboxymethylhistidinate). The reaction profiles depicted by the absorbance change in the UV–vis spectrum show a sigmoid shape with an induction period. The induction period is reduced by the addition of acid, fluoride, thiocyanate, VO^{2+}, VO_2^+, and trolox compared to the solution containing perchlorate. On the other hand, the induction period was elongated by the addition of chloride, bromide, and 2-*tert*-butyl-*p*-cresol. These behaviors are discussed on the basis of a radical chain mechanism. The self-decomposition reactions have also been followed by the ^1H and ^{51}V NMR and EPR spectra. These spectral studies as well as the UV–vis spectral study indicate that vanadium(V) is partly reduced to vanadium(IV) in the self-decomposition process. The histada complex yields a mixed-valence dinuclear complex in a concentrated solution, and the dpot complex yields a mixed-valence tetranuclear complex. The reduction of vanadium ion suggests that the peroxo ligand may act as a reducing agent. In order to know the fate of the peroxo ligand, we tried to detect superoxide anion and hydroxyl radical, which were anticipated to be produced in the self-decomposition process. The formation of superoxide anion was spectrophotometrically confirmed using two independent methods, including the reduction of cytochrome *c* and the reduction of sodium 4-[3-(iodophenyl)-2-(4-nitrophenyl)-2*H*-5-tetrazolio]-1,3-benzene disulfonate (WST-1). The formation of hydroxyl radical was confirmed by an EPR spin trapping technique. The oxidizing abilities of the peroxovanadium(V) complexes toward bovine serum albumin (BSA) were also evaluated. In the protein carbonyl assay, it was found that the total amount of protein carbonyl in BSA was increased by the reaction with the peroxovanadium complexes in the concentration-dependent manner. In addition, the oxidation of sulfhydryl group in BSA induced by the peroxovanadium complexes was confirmed.

Introduction

Peroxovanadium(V) species, as known for relevant species in a classical spot test for vanadate, have been receiving renewed attention with regard to their biological significance.[2] Peroxovanadium(V) species have been demonstrated to be an important intermediate in the enzymatic process of vanadium-dependent haloperoxidases (VHPO) isolated from

* To whom correspondence should be addressed. E-mail: kanamori@sci.toyama-u.ac.jp.
† Toyama University.
‡ University of Tsukuba.
§ Nara Women's University.
|| University of Yamanashi.

(1) Part 2: Reactivity and Mechanism of Bromide Oxidation as Function Models Bromoperoxidases. The manuscript will appear elsewhere.
(2) (a) *Vanadium in Biological Systems*; Chasteen, N. D., Ed.; Kluwer Academic Publishers: Dordrecht, The Netherlands, 1990. (b) *Metal Ions in Biological Systems: Vanadium and its role in life*; Sigel, H., Sigel, A., Eds.; Marcel Dekker: New York, 1995; Vol. 31. (c) *Vanadium in the Environment*; Nriagu, J. O., Ed.; John Wiley: New York, 1998.

10.1021/ic030292f CCC: $27.50 © 2004 American Chemical Society
Published on Web 10/06/2004

marine algae and terrestrial fungi and catalyze the halogenation of organic substrates via the oxidation of halides by hydrogen peroxide.[3] Several peroxovanadium(V) complexes with a hetero ligand have been prepared as model compounds, and their VHPO-like reactions have bee investigated.[4] Peroxovanadium(V) complexes have also been utilized as oxidizing agents in preparative organic chemistry.[5] However, it has been known that the chemistry of peroxovanadium(V) complexes is more complex than that of Fenton-like systems.[6]

Peroxovanadium(V) species have also attracted the attention of pharmacologists with respect to their insulin mimetic functions.[7,8] Namely, vanadium(V) exerts insulin-mimetic activities in a synergistic manner with peroxide.[9] Peroxovanadium(V) species formed in vivo have been considered to be relevant to insulin mimesis.[10] It has been demonstrated that discrete peroxovanadium(V) complexes are also effective insulin mimics.[11−13] However, it is anticipated that chemistry of the insulin mimetic activities of peroxovanadium(V) complexes is also very complex mainly because of the easy redox interplay between vanadium(V) and vanadium(IV), the stereochemical nonrigidity of vanadium(V) species, and the lability of the ligand at coordination sites.[14]

In order to understand the complex physiological behavior of peroxovanadium(V) complexes, it is necessary to know the properties of peroxovanadium(V) complexes in solution. One of the most interesting features of peroxovanadium(V) complexes in solution should be their self-decomposition reactions. The stability of peroxovanadium(V) complexes strongly depends on the coexisting hetero ligand. For example, $[VO(O_2)(pda)]^-$ (pda, *N*-pyridylmethyliminodiacetate) is very stable in an acidic solution while $[VO(O_2)(cmhist)]^-$ (cmhist, *N*-carboxymethylhistidine) slowly decomposes in the same condition, though both complexes have a similar donor atom set.[13] We have shown that the latter complex exhibits weak but definitive insulin-mimetic activity in vitro while the former complex never does.[13] This finding suggested that the products formed in the self-decomposition reaction may be relevant to the insulin mimetic activity of the peroxovanadium(V) complexes previously studied. These circumstances about peroxovanadium(V) complexes prompted us to investigate the self-decomposition reaction of peroxovanadium(V) complexes in detail.

The self-decomposition reaction of peroxovanadium(V) species has been studied so far using ^{51}V NMR spectroscopy[15] and the combined method of EPR, UV−vis spectrometries, and iodometry.[6] Reaction mechanisms concerning the self-decomposition reaction have been presented mainly on the basis of the kinetic analysis.[6] In this paper, we report the detailed study on the self-decomposition reaction of the mononuclear complexes, $[VO(O_2)(histada)]^-$ and $[VO(O_2)(cmhist)]^-$, and the dinuclear complex, $[(VO)_2(O_2)_2(dpot)]^{3-}$, to reveal the factors affecting the decomposition profiles using UV−vis, ^1H and ^{51}V NMR, and EPR spectrophotometries. It has been indicated that vanadium(V) can be reduced to vanadium(IV) in the self-decomposition process.[6,16−19] We have also indicated in a previous paper that the self-decomposition reaction of $[VO(O_2)(cmhist)]^-$ accompanies the reduction of vanadium(V) to vanadium(IV).[13] However, the self-decomposition reactions have been followed only by the decrease of the absorbance due to the peroxo CT transition observed around 450 nm as far as we know. We have been able to follow the decomposition of the V(V)−peroxo moiety and the reduction of V(V) to V(IV) simultaneously using a new dimeric peroxovanadium(V) complex, $[(VO)_2(O_2)_2(dpot)]^{3-}$, and a concentrated aqueous solution of $[VO(O_2)(histada)]^-$ and $[VO(O_2)(cmhist)]^-$. The reduction of vanadium(V) suggests that the peroxo group in the complex may act as a reducing agent. Thus, we tried to identify the active oxygen species generated in the self-decomposition process of the peroxovanadium(V) complexes. We also examined the oxidizing ability of the peroxovanadium(V) complexes using bovine serum albumin (BSA).

Experimental Section

Materials. Potassium (*N*-carboxymethylhistidinato)oxoperoxovanadate(V), $K[VO(O_2)(cmhist)]\cdot H_2O$, was prepared according to the literature method.[13] WST-1 (sodium 4-[3-(iodophenyl)-2-(4-nitrophenyl)-2*H*-5-tetrazolio]-1,3-benzene disulfonate) and SOD (superoxide dismutase) were purchased from Wako Chemicals (Osaka, Japan). BSA (bovine serum albumin) was purchased from Sigma Chemical (St. Louis, MO). DTPA (diethylenetriaminepentaacetic acid) and SDS (sodium *n*-dodecyl sulfate) were purchased from Kanto Chemical (Tokyo, Japan). DMPO (5,5-dimethyl-1-pyrroline-*N*-oxide) was purchased from Dojindo Laboratories (Kumamoto, Japan). Cytochrome *c* from horse heart, DNPH (2,4-dinitrophenylhydrazine), DTNB [5,5′-dithiobis(2-nitrobenzoic acid)],

(3) (a) Vilter, H. Vanadium-Dependent Haloperoxidase. In *Metal Ions in Biological Systems: Vanadium and its role in life*; Sigel, H., Sigel, A., Eds.; Marcel Dekker: New York, 1995; Vol. 31. (b) Wever, R.; Hemrica, W. Vanadium in Enzymes. In *Vanadium in the Environment*; Nriagu, J. O., Ed.; John Wiley: New York, 1998. (c) Rehder, D.; Santoni, G.; Licini, G. M.; Schuzke, V.; Meier, B. *Coord. Chem. Rev.* **2003**, *237*, 53.

(4) (a) Butler, A.; Walker, J. V. *Chem. Rev.* **1993**, *93*, 1037. (b) Butler, A.; Clague, M. J.; Meister, G. E. *Chem. Rev.* **1994**, *94*, 625.

(5) Hirao, T. *Chem. Rev.* **1997**, *97*, 2797.

(6) Bonchio, M.; Conte, V.; Di Furia, F.; Modena, G.; Moro, S.; Edwards, J. O. *Inorg. Chem.* **1994**, *33*, 1631.

(7) Rehder, D.; Costa Pesoa, J.; Geraldes, C. F. G. C.; Castro, M. M. C. A.; Kabanos, T.; Kiss, T.; Meier, B.; Micela, G.; Pettersson, L.; Rangel, M.; Salifoglou, A.; Wang, D. *J. Biol. Inorg. Chem.* **2002**, *7*, 384.

(8) Thompson, K. H.; McNeill, J. H.; Orvig, C. *Chem. Rev.* **1999**, *99*, 2561.

(9) Kadota, S.; Fantus, I. G.; Deragon, G.; Cuyda, H. J.; Posner, B. I. *J. Biol. Chem.* **1978**, *262*, 8252.

(10) Fantus, I. G.; Kadota, S.; Deragon, G.; Foster, B.; Posner, B. I. *Biochemistry* **1989**, *28*, 8864.

(11) Shaver, A.; Ng, J. B.; Hall, D. A.; Lum, B. S.; Posner, B. I. *Inorg. Chem.* **1993**, *32*, 3109.

(12) Posner, B. I.; Faure, R.; Burgess, J. W.; Bevan, A. P.; Lachance, D.; Z-Sun, G.; Fantus, I. G.; Ng, J. B.; Hall, D. A.; Lum, B. S.; Shaver, A. *J. Biol. Chem.* **1994**, *269*, 4596.

(13) Kanamori, K.; Nishida, K.; Miyata, N.; Okamoto, K.; Miyoshi, Y.; Tamura, A.; Sakurai, H. *J. Inorg. Biochem.* **2001**, *86*, 649.

(14) Djordjevic, C.; Vuletic, N.; Renslo, M. L.; Puryear, B. C.; Alimard, R. *Mol. Cell. Biochem.* **1995**, *153*, 25.

(15) Conte, V.; Di Furia, F.; Moro, S. *J. Mol. Catal. A: Chem.* **1997**, *120*, 93.

(16) Thompson, R. C. *Inorg. Chem.* **1983**, *22*, 584.

(17) Mimoun, H.; Saussine, L.; Daire, E.; Postal, M.; Fischer, J.; Weiss, R. *J. Am. Chem. Soc.* **1983**, *105*, 3101.

(18) (a) Djordjevic, C.; Vuletic, N.; Renslo, M. L.; Puryear, B. C.; Alimard, R. *Moll. Cell Biochem.* **1985**, *153*, 25. (b) Djordjevic, C.; Wampler, G. L. *J. Inorg. Biochem.* **1985**, *25*, 51.

(19) Shi, X.; Dalal, N. S. *Arch. Biochem. Biophys.* **1993**, *307*, 336.

and TCA (trichloroacetic acid) were purchased from nacalai tesque (Kyoto, Japan). The protein assay kit was purchased from Bio-Rad (Tokyo, Japan).

Synthesis of Barium Histamine-*N,N*-diacetate (Bahistada). To the solution of monochloroacetic acid (18.9 g, 0.2 mol) in 50 mL of water was added solid $LiOH·H_2O$ (8.39 g, 0.2 mol) in limited amounts. The solution temperature was kept below 10 °C during this procedure. Histamine dihydrochloride (18.4 g, 0.1 mol) was dissolved in 30 mL of water, and then solid $LiOH·H_2O$ (8.39 g, 0.2 mol) in limited amounts was added below 10 °C to neutralize the solution. The mixture of this solution with the monochloroacetate solution was stirred at room temperature until the pH of the solution did not vary. Solid $LiOH·H_2O$ (8.39 g, 0.2 mol) in limited amounts was added to the solution at 40 °C with stirring while keeping the pH of the solution from exceeding 11. This procedure took about 1 week. After the addition of the lithium hydroxide was finished, the solution was stirred at room temperature for an additional 1 day. Then, barium perchlorate (33.62 g, 0.1 mol) was added, and the mixture was kept stirring for 4 h. After the pH of the solution was adjusted to 11 by adding 6 M NaOH, ethanol was added until the solution became cloudy. The solution was kept in a refrigerator to yield a white mass. The crude product was collected by filtration and suspended in a 1:1 mixture of water and ethanol. The suspension was stirred for a while to dissolve contaminated LiCl. The white precipitate was filtered, washed with ethanol, and air-dried. Yield 22.6 g (54%). Anal. Calcd for $C_9H_{11}N_3O_4Ba·0.5H_2O·LiCl$: C, 26.11, H, 2.92, N, 10.15. Found: 26.22, H, 2.86, N, 10.04. An equivalent amount of LiCl contaminated in the final product was not able to be removed even after successive washing. Selected IR data (KBr, cm^{-1}): 1564(vs) ($\nu_{as}(CO_2)$), 1403(s) ($\nu_s(CO_2)$), 1344(m), 1330(m), 1266(m), 1243(m), 1119(s), 1004(m), 976(m), 938(m), 902(m), 857(m), 809(m), 750(m), 717(m), 663(m).

Synthesis of $Cs_3[(VO)_2(O_2)_2(dpot)]·3H_2O$. Vanadium(V) oxide (0.91 g, 5 mmol) was suspended in 20 mL of water, and cesium carbonate (4.22 g, 7.5 mmol) was added. Stirring this suspension at 60 °C resulted in a clear solution. After the solution was cooled in an ice bath, 1,3-diamino-2-propanol-*N,N,N′,N′*-tetraacetic acid, H_5dpot (1.61 g, 5 mmol), and 10% hydrogen peroxide (1.7 mL, 5 mmol) were added. The mixture was stirred at 0 °C for an hour to give a dark red solution. Dark red crystals were obtained by adding methanol to the solution. Yield: 3.1 g (64%). Anal. Calcd for $C_{11}H_{19}N_2O_{18}Cs_3V_2$: C, 13.65; H, 1.98; N, 2.90. Found: C, 13.85; H, 1.91; N, 2.92. Selected IR data (KBr, cm^{-1}): 1646(vs) ($\nu_{as}(CO_2)$), 1440(m) ($\nu_s(CO_2)$), 1402(s), 1270(m), 1092(m), 1054(m), 973(m), 935(s) (ν(V═O)), 909(s), 885(s), 734(m), 564(m).

Synthesis of $Na[VO(O_2)(histada)]·3.75H_2O$. Vanadium(V) oxide (0.36 g, 2 mmol) was dissolved in 30 mL of water by adding 4 mL of 1 M NaOH (4 mmol) with heating and stirring. Bahistada·$0.5H_2O·$LiCl (1.65 g, 4 mmol) was added to 8 mL of 0.5 M H_2SO_4 (4 mmol). $BaSO_4$ that precipitated was filtered off. The filtrate was added to the vanadium(V) solution followed by the addition of 1.4 mL of 10% hydrogen peroxide. After stirring the mixture for 1 h, a red solution resulted that was concentrated to dryness with a rotary evaporator. The crude product was dissolved in a small amount of water. Allowing the solution to sit in a refrigerator afforded red crystals. Yield 0.45 g (27%). Anal. Calcd for $C_9H_{11}N_3O_7VNa·3.75H_2O$: C, 26.06; H, 4.50; N, 10.13. Found: C, 26.00; H, 4.26; N, 10.10. Selected IR data (KBr, cm^{-1}): 1615(vs) ($\nu_{as}(CO_2)$), 1394(s) ($\nu_s(CO_2)$), 1270(m), 1086(m), 1029(m), 947(s) (ν(V═O), 855(m), 618(m).

SAFETY NOTE! Although no problems were encountered during the concentration of the reaction solution, the solution containing peroxide is potentially explosive and should be handled in small quantities with care.

X-ray Structure Determination. A crystal was mounted on a glass fiber, coated with epoxy as a precaution against solvent loss, and centered on an Enraf-Nonius CAD-4 diffractometer using graphite-monochromated Mo Kα radiation. The unit-cell parameters were determined by a least-squares refinement, using the setting angles in the range $41° < 2\theta < 47°$. Data reduction and the application of Lorentz polarization, the linear decay correction, and the empirical absorption correction on a series of ψ scans were carried out. The structure was solved by a direct method (SIR 92)[20] and conventional difference Fourier techniques. The structure was refined by full-matrix least-squares techniques on *F*. All non-hydrogen atoms were anisotropically refined. All of the calculations were performed on an INDIGO II computer using the crystallographic package TEXAN.[21]

Physical Methods. UV−vis spectra were recorded using a Shimadzu UV-3100PC spectrophotometer or a Perkin-Elmer UV−vis spectrometer Lamda Bio 20. IR spectra (KBr disk) were measured using a JASCO FT-IR8000. EPR spectra were obtained with a JEOL JES-RE1 or a JEOL JES-TE200 spectrometer. ^1H and ^{51}V NMR spectra were recorded on a JEOL α-400 spectrometer.

Detection of Superoxide Anion ($O_2^{\bullet-}$). Method Utilizing Reduction of Cytochrome *c*. The amount of superoxide anion produced in the self-decomposition process of the cmhist complex was estimated by measuring the increase of the absorbance of the 550 nm band specific to the reduced form of cytochrome *c* (Fe^{2+}).[22] The concentration of decomposed complex was calculated from the decrease of the absorbance of the 430 nm band due to the peroxo CT transition. As it was found that about 12% of the cmhist complex decomposed within 15 min after dissolving the complex in phosphate buffered-solution (pH 7.4), we set up the reaction time of the oxidized form of cytochrome *c* with the cmhist complex in 15 min.[23]

The cmhist complex was dissolved in 50 mM sodium phosphate buffer (pH 7.4) to give 5 mM aqueous solution of the cmhist complex. Cytochrome *c* and SOD were dissolved in deionized water (>18 MΩ) to give 2 and 15.6 mM solutions, respectively. The cmhist complex solution was added to the cytochrome *c* solution in 50 mM phosphate buffer (pH 7.4). The final concentrations of the cmhist complex and cytochrome *c* were 1 and 30 mM, respectively. After the reaction mixtures stood for 15 min at room temperature, the absorbance of the 550 nm band (ϵ = 19.1 $mM^{-1}cm^{-1}$) was measured by a UV−vis spectrophotometer. For a control experiment, the cmhist complex (1 mM) was reacted with cytochrome *c* (30 mM) in the presence of SOD (final concentration 0.1 mM) for the same time period described. The concentration of superoxide anion produced in the self-decomposition process of the cmhist complex was calculated by subtracting the absorbance at 550 nm of the control sample from that of the test sample.

Method Utilizing Reduction of WST-1. The WST-1 method, which utilizes the reduction of WST-1 to WST-1 formazan by superoxide anion, was also used to estimate the amount of the superoxide anion produced in the self-decomposition.[24]

(20) *SIR 92*: Altomare, A.; Burla, M. C.; Camalli, M.; Cascarano, M.; Giacovazzo, C.; Guagliardi, A.; Polidori, G. *J. Appl. Crystallogr*. **1994**, *27*, 435.
(21) *TEXAN*, *Single-Crystal Structure Analysis Software*, version 1.10; Molecular Structure Corporation: The Woodlands, TX, 1997.
(22) Butler, J.; Jayson, G. G.; Swallow, A. J. *Biochim. Biophys. Acta* **1975**, *488*, 215.
(23) Since the reduced form of cytochrome *c* is fairly unstable and the 550-nm band disappeared when the reaction solution allowed to stand for a long period, we limited the measurement time to 15 min.

Solutions (5 mM) of the peroxovanadium(V) complexes and of WST-1 (10 mM) were prepared using 50 mM sodium phosphate buffer (pH 7.4). Both solutions were mixed in the same buffer to give the final concentrations of 500 μM. The reaction mixtures stood for 48 h for the cmhist and histada complexes and 4 h for the dpot complex at 37 °C. Subsequently, the absorbance of the 438 nm band, which is characteristic of WST-1 formazan ($\epsilon = 37000$), of the reaction mixture was measured by UV−vis spectrophotometer. For control experiments, the vanadium solution as well as the WST-1 solution of 500 μM was also stood for the same time period. These solutions were used as control experiments. The amount of decomposed complex was calculated from the decrease of the peroxo CT band intensity.

Detection of Hydroxyl Radical (OH$^{\bullet}$). The hydroxyl radical produced in the self-decomposition process of the peroxovanadium(V) complex was determined by an EPR spin trapping technique using DMPO as a spin trap reagent.[25] Briefly, each peroxovanadium(V) complex and DTPA were dissolved in 50 mM sodium phosphate buffer (pH 7.4) to give an 80 mM solution for the cmhist and histada complexes, a 150 mM solution for the dpot complex, and a 10 mM solution for DTPA. The stock solution of DMPO (10.98 M) was used without making any further dilutions and purifications. The final concentrations of the cmhist, histada, and dpot samples and DMPO were adjusted to 75.5, 75.5, 100, and 610 mM, respectively, by mixing appropriate amounts of each complex solution and the DMPO solution. After the reaction mixture stood for several minutes at room temperature, the aliquot (50 μL) of this solution was transferred to a capillary tube, and then the end of the capillary tube was sealed with silicon paste. The sealed capillary tube was put into the cavity of EPR apparatus. EPR spectra of the reaction mixtures were measured under the following conditions: microwave power, 8 mW; microwave frequency, 9.20 GHz; modulation amplitude, 0.1 mT; time constant, 0.1 s; sweep time, 2 min; center fields, 327 ± 5 mT.[25]

Evaluation of Oxidizing Ability to Protein. Protein Carbonyl Assay. When several amino acid residues in protein such as lysine and serine were oxidized, protein carbonyls are produced. Reaction of the carbonyl group and 2,4-dinitrophenylhydrazine (DNPH) yields 2,4-dinitrophenylhydrazone derivatives, which exhibit an absorption maximum at 370 nm ($\epsilon = 22000$).[25] Amounts of the amino acid residues oxidized by the reaction with the peroxovanadium(V) complexes were estimated on the basis of the absorbance change at 370 nm. The amount of decomposed complex was calculated on the basis of the decrease of the absorbance in the peroxo CT transition region of each vanadium complex.

At 37 °C, BSA (1 mg/mL) was reacted with a 3 mM solution of the cmhist and histada complexes or 1−5 mM solutions of the dpot complex in 50 mM phosphate buffer (pH 7.4) for 48 h for the cmhist and histada complexes, or 1 h for the dpot complex. Ethanol (4 mL) was then added to the reaction mixtures in order to precipitate the protein. Vanadium species remained in the aqueous layer. After centrifugation at 3000 rpm for 20 min, the supernatant including vanadium species was removed by decantation. After the precipitate was dried in a dryer at 37 °C for 90 min, it was dissolved in 1 mL of 50 mM phosphate buffer (pH 7.4). Then, 200 μL of 10 mM DNPH solution in 2 M HCl was added to the solution, and the mixture continued standing at room temperature for 1 h. Precipitate containing modified BSA was deposited by adding 1.2 mL of 20% TCA aqueous solution. After centrifugation at 3000 rpm for 20 min, the supernatant was removed to leave the pellet (BSA pellet). In order to remove the nonreacted DNPH contaminated in the BSA pellet, the pellet was washed twice with 2 mL of an ethyl alcohol/ethyl acetate (1:1) mixture. The BSA pellet was dried at 37 °C for 90 min followed by dissolution in 2 mL of 50 mM phosphate buffer (pH 7.4). An aliquot (100 mL) of the solution was used for protein assay.

Table 1. Crystallographic Data for $Cs_3[(VO)_2(O_2)_2(dpot)]\cdot 3H_2O$

formula	$C_{11}H_{19}N_2O_{18}Cs_3V_2$
fw	967.88
T, K	296
λ(Mo Kα), Å	0.7107
cryst syst	monoclinic
space group	$P2_1/n$
a, Å	9.885(1)
b, Å	26.997(3)
c, Å	9.929(1)
β, deg	113.03(1)
V, Å^3	2438.6(5)
Z	4
D_{calcd}, g cm^{-3}	2.64
μ, cm^{-1}	52.7
F(000)	1816
R^a	0.056
$R_w^{b,c}$	0.157

[a] $R = \sum(|F_o| - |F_c|)/\sum(|F_o|)$. [b] $R_w = (\sum w(|F_o| - |F_c|)^2/\sum w(|F_o|^2)^{1/2}$. [c] $w = 4(F_o)^2/s^2(F_o)$.

Protein Sulfhydryl Assay. Sulfhydryl assay was carried out according to the literature procedure.[26] Briefly, BSA (2 mg/mL) was reacted with the 50−150 mM solutions of the dpot complex in 50 mM phosphate buffer (pH 7.4) at 37 °C for 1 h. Then, 200 μL of 2 M HCl was added to the reaction mixture, followed by the addition of 700 μL of 3% SDS aqueous solution. The reaction mixture was kept standing at room temperature for 5 min. Precipitate containing modified BSA was deposited by addition of 2 mL of ethanol and then 2 mL of hexane. The mixture was centrifuged at 3000 rpm for 20 min, and then precipitate (BSA pellet) was collected. The BSA pellet was washed twice with the mixture of ethyl alcohol and ethyl acetate (1:1). The pellet was dried at 37 °C for 90 min, and then dissolved in 1 mL of 50 mM sodium phosphate buffer containing 2% of SDS (pH 8.0). After 100 μL of 4 mM DTNB solution in 50 mM sodium phosphate buffer was added to the solution and the mixture stood for 30 min, a UV−vis spectrum of the mixture was measured. An aliquot (50 μL) of the mixture was used for the determination of the remaining protein amounts in the mixture. The amount of the sulfhydryl group remaining in the modified BSA was determined using 5,5′-dithiobis-(2-nitrobenzoic acid) (DTNB) assay utilizing the specific absorption at 412 nm ($\epsilon = 13600$ M^{-1} cm^{-1}).

Protein Assay. In the case of the protein carbonyl assay, the amount of the remaining intact protein in the modified BSA sample was determined using a protein assay kit (Bradford assay). The amount of the remaining intact protein in the modified BSA sample was determined using DC protein assay kit (Lowry assay) for the protein sulfhydryl assay.

Results and Discussion

Structure of Complexes. The structure of $Cs_3[(VO)_2(O_2)_2(dpot)]\cdot 3H_2O$ was determined by a single-crystal X-ray analysis. The crystallographic data are summarized in Table 1. The selected bond distances and angles are listed in Table

(24) Ukeda, H.; Kawana, D.; Maeda, S.; Sawamura, M. *Biosci. Biotechnol. Biochem.* **1999**, *66*, 485.
(25) (a) Matsugo, S.; Yan, L. J.; Han, D.; Trischler, H. J.; Packer, L. *Biochem. Biophys. Res. Commun.* **1995**, *208*, 161. (b) Ali, M. A.; Yasui, F.; Matsugo, S.; Konishi, T. *Free Rad. Res.* **2000**, *32*, 485.
(26) Frank, T. *Anal. Biochem.* **1969**, *27*, 502.

Table 2. Selected Bond Distances (Å) and Angles (deg) for $Cs_3[(VO)_2(O_2)_2(dpot)]\cdot 3H_2O$

V1−O1	2.031(5)	V2−O7	2.029(5)
V1−O3	2.175(4)	V2−O5	2.176(4)
V1−O9	2.087(4)	V2−O9	2.087(4)
V1−O10	1.608(5)	V2−O11	1.613(5)
V1−O12	1.83(1)	V2−O15	1.842(8)
V1−O13	1.759(8)	V2−O14	1.795(7)
V1−N1	2.246(5)	V2−N2	2.209(5)
O1−V1−O3	85.6(2)	O7−V2−O5	84.8(2)
O1−V1−O9	151.7(2)	O7−V2−O9	152.1(2)
O1−V1−O10	93.7(3)	O7−V2−O11	93.6(2)
O1−V1−O12	78.1(5)	O7−V2−O15	77.7(3)
O1−V1−O13	115.0(4)	O7−V2−O14	116.9(3)
O1−V1−N1	73.2(2)	O7−V2−N2	73.4(2)
O3−V1−O9	82.3(2)	O5−V2−O9	82.1(2)
O3−V1−O10	167.6(2)	O5−V2−O11	167.4(2)
O3−V1−O12	85.5(4)	O5−V2−O15	88.0(3)
O3−V1−O13	87.1(3)	O5−V2−O14	87.9(2)
O3−V1−N1	75.4(2)	O5−V2−N2	75.2(2)
O9−V1−O10	92.8(2)	O9−V2−O11	93.9(2)
O9−V1−O12	126.0(4)	O9−V2−O15	126.0(3)
O9−V1−O13	89.9(4)	O9−V2−O14	87.1(3)
O9−V1−N1	79.1(2)	O9−V2−N2	79.5(2)
O10−V1−O12	106.4(4)	O11−V2−O15	103.9(3)
O10−V1−O13	104.3(3)	O11−V2−O14	103.9(3)
O10−V1−N1	92.5(2)	O11−V2−N2	92.4(2)
O12−V1−O13	36.9(4)	O15−V2−O14	39.4(3)
O12−V1−N1	146.4(4)	O15−V2−N2	147.6(3)
O13−V1−N1	160.4(3)	O14−V2−N2	159.6(3)

2. The dpot complex takes a dinuclear structure bridged by a central alkoxo group of $dpot^{5-}$ as shown in Figure 1. The complex is approximately symmetric with respect to the quasi-mirror-plane through O9 and C10 atoms. Each vanadium atom adopts a pentagonal bipyramidal structure commonly found in monoperoxovanadium(V) complexes with a multidentate chelate ligand.[4b] The pentagonal plane is completed by an amine nitrogen atom (N1 or N2), a carboxylato oxygen atom (O1 or O7), an alkoxo oxygen atom (O9), and two peroxo oxygen atoms. The two peroxo groups coordinate side by side in the adjacent positions. These peroxo groups are, however, fluctuated in each position as shown by their large thermal ellipsoids. Therefore, the bond distances and angles around the peroxo groups could not be determined precisely and were omitted in Table 2. The low temperature X-ray crystal analysis was tried unsuccessfully since the crystallographic system changed from monoclinic to triclinic. The V1−O3 and V2−O5 bond lengths are long reflecting a strong trans influence of the oxo groups. Other bond distances and angles are in the normal range.

Two dinuclear peroxovanadium(V) complexes containing an organic ligand, $K_2[\{VO(O_2)(citrato)\}_2]\cdot 2H_2O$[27] and $K_2[\{VO(O_2)(lactato)\}_2]$,[28] have been structurally characterized. In contrast to the adjacent arrangement in the dpot complex, the two peroxo groups in these complexes are situated in the distal positions. Bonchio et al.[6] have proposed that a dinuclear intermediate plays an important role in the self-decomposition reaction process of the monoperoxovanadium(V) complexes. Namely, the intramolecular electron transfer from a peroxo group in one mononuclear unit to a peroxo group in another mononuclear unit has been considered to be a key step in the self-decomposition reaction of $[VO(O_2)(pic)(H_2O)_2]$ based on the kinetic analysis. In this regard, the present dinuclear dpot complex is considered to mimic the postulated dinuclear intermediate more appropriately than the citrate and lactate complexes.

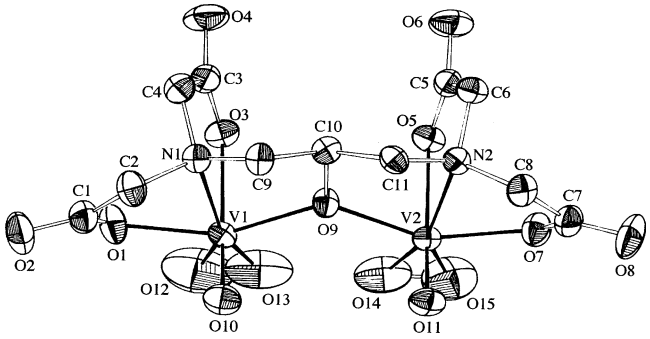

Figure 1. ORTEP drawing of $[(VO)_2(O_2)_2(dpot)]^{3-}$ with the atom numbering scheme.

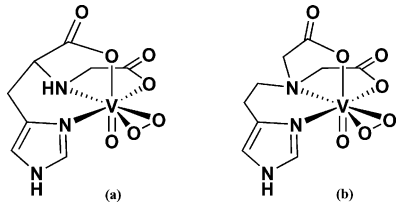

Figure 2. Schematic presentation of the structure of $[VO(O_2)(cmhist)]^-$ (a) and the proposed structure for $[VO(O_2)(histada)]^-$ (b).

The structure of the cmhist complex has been published in our previous paper[13] and is shown schematically in Figure 2a. We could not obtain the crystals of the histada complex with a quality good enough for a single-crystal X-ray analysis. We thus propose the structure of the histada complex to be similar to that of the cmhist complex as shown in Figure 2b. The proposed structure is consistent with the preliminary X-ray result (R = 21% level) of the histada complex. The histada and cmhist complexes can be regarded as a model complex of the active site of the vanadium-dependent haloperoxidase with regard to the situation that the imidazole group coordinates in the cis position of the peroxo group, though the coordination number is different from that of the enzyme (7 vs 5).[29]

General Tendencies of the Self-Decomposition Reaction. The self-decomposition reaction of the dpot complex was followed by taking the UV−vis spectrum every 1 h. Figure 3 shows the time-dependent UV−vis spectrum until 20 h under the condition described in the figure legend. Perchlorate was employed to adjust the ionic strength of the solution since its coordination ability is very small, it may not take part in the reduction of vanadium(V), it cannot be oxidized anymore by peroxide, and thus it can be considered to be innocent in the self-decomposition reaction. The ligand-to-metal charge transfer (LMCT) band at 430 nm due to the coordinated peroxo group decreases slowly with time, indicating that the peroxo group dissociates from the first coordination sphere or decomposes into some other species.

(27) Djordjevic, C.; Lee, M.; Sinn, E. *Inorg. Chem*. **1989**, *28*, 719.
(28) Demartin, F.; Biagioli, M.; Strinna-Erre, L.; Panzanelli, A.; Micera, G. *Inorg. Chim. Acta* **2000**, *299*, 123.
(29) Messerschmidt, A.; Prade, L.; Wever, R. *Biol. Chem*. **1997**, *378*, 309.

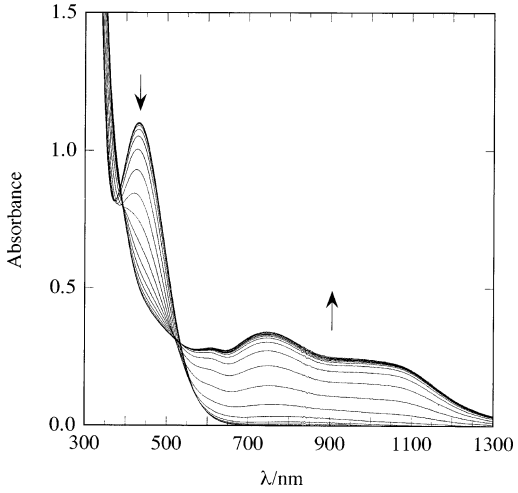

Figure 3. Successive UV−vis absorption spectra of $Cs_3[(VO)_2(O_2)_2(dpot)]\cdot 3H_2O$ observed at 1-h intervals. Conditions: [complex] = 3.5 mM, pH 4.51 ($HClO_4$), ionic strength = 1.0 M (by $NaClO_4$), 30 °C.

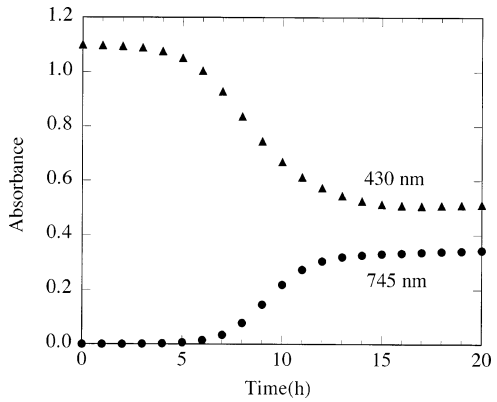

Figure 4. Time dependence of the absorption intensities at 430 and 745 nm for $Cs_3[(VO)_2(O_2)_2(dpot)]\cdot 3H_2O$. Conditions: [complex] = 3.5 mM, pH 4.51 ($HClO_4$), ionic strength = 1.0 M (by $NaClO_4$), 30 °C.

Accompanying the decrease of the intensity of the peroxo LMCT band, the intense bands appear in the 600−1300 nm region. These intense bands are characteristic of the mixed valence V^V/V^{IV} dinuclear vanadium complex and have been assigned to the intervalence charge-transfer transition.[30] This observation, thus, suggests that vanadium(V) in the starting dpot complex is partly reduced to vanadium(IV) in the self-decomposition process. The partial reduction of vanadium(V) was confirmed by the structure of the decomposition product, which has been proven to be the tetranuclear mixed-valence $V^V{}_2V^{IV}{}_2$ complex, $[V_4O_4(\mu\text{-}O)_2(dpot)_2]^{4-}$.[31]

The absorbance values at 430 and 745 nm are plotted as a function of the reaction time in Figure 4. The intensity of the peroxo LMCT band decreases very slowly until ca. 5 h. The decreasing rate becomes faster after 5 h, and the absorbance converges to the constant value after 15 h. The intensity of the intervalence CT band increases accompanying with a decrease in the intensity of the peroxo CT band. Thus, the reaction profiles depicted by the absorbance of the peroxo CT band as well as the intervalence CT band show the sigmoid curve with the induction period, which is usually noticed in an autocatalytic reaction. The similar reaction profile has been reported for the self-decomposition reaction of $[VO(O_2)(pic)(H_2O)_2]$, and the induction period has been considered to be the period until the full radical chain reaction starts.[6] It should be noticed that there is a time lag between the appearance of the intervalence CT band and the disappearance of the peroxo CT band. The time to reach the midpoint in the absorbance change of the intervalence band is delayed ca. 0.9 h from that of the peroxo CT band. Namely, the formation of the mixed-valence complex is initiated after the peroxo group dissociates from the coordination sphere to some extent.

In order to examine whether a reduction of vanadium(V) would occur in the absence of peroxide and to what extent, if it would occur, the spectral change was also followed for the vanadium(V)−dpot system without peroxo groups using a solution containing Na_3VO_4 and $dpot^{5-}$ at pH 4.58. The results showed that the reduction occurs spontaneously even without a peroxo ligand but the reduction rate is extremely slow compared with the peroxo complex. Thus, the absorbance of the intervalence CT band only increased by 0.06 even after 50 h. Therefore, it can be concluded that the reduction of vanadium(V) in the dpot complex is primarily caused by the peroxo group.

In our previous paper,[13] we showed that the peroxo CT band of the cmhist complex decreases with time in an acidic solution as in the case of the dpot complex. In the previous experiment, however, we could not confirm the reduction of vanadium(V) in the UV−vis spectral change since we used a diluted solution (3.5 mM). We, therefore, reinvestigated the UV−vis spectral change of the cmhist complex as well as the related histada complex using a concentrated solution (50 mM for the cmhist complex and 100 mM for the histada complex) and a cell of 1 mm light-path length. The observed spectral changes are shown in Figure 5. The histada complex exhibits the spectral change that is very similar to that of the dpot complex, indicating that vanadium(V) is partly reduced to vanadium(IV) to yield the mixed-valence complex as for the dpot complex. The reduction of vanadium(V) was also verified for the cmhist complex. However, we cannot affirm the formation of the mixed-valence complex since the absorbance in the intervalence CT transition region of the cmhist complex is weak compared to the histada complex. The weak intervalence CT band of the cmhist complex may be due to the lower solubility of the cmhist complex, which results in less extent of dimerization. Perhaps the association constant between the mononuclear V(V) and V(IV) complexes with cmhist might be lower compared to the histada complexes.

As for the decomposition product of the peroxovanadium(V) complexes, the present results are different from those obtained in the previous work. Thus, a di(μ-oxo)vanadium(V) complex was obtained as a decomposition product of $[VO(O_2)(pic)(H_2O)_2]$,[6,17] whereas vanadium(V) was partly reduced to vanadium(IV) for the present complexes. This

(30) Kojima, A.; Okazaki, K.; Ooi, S.; Saito, K. *Inorg. Chem.* **1983**, *22*, 1168.
(31) Kumagai, H.; Kawata, S.; Kitagawa, S.; Kanamori, K.; Okamoto, K. *Chem. Lett.* **1997**, 249.

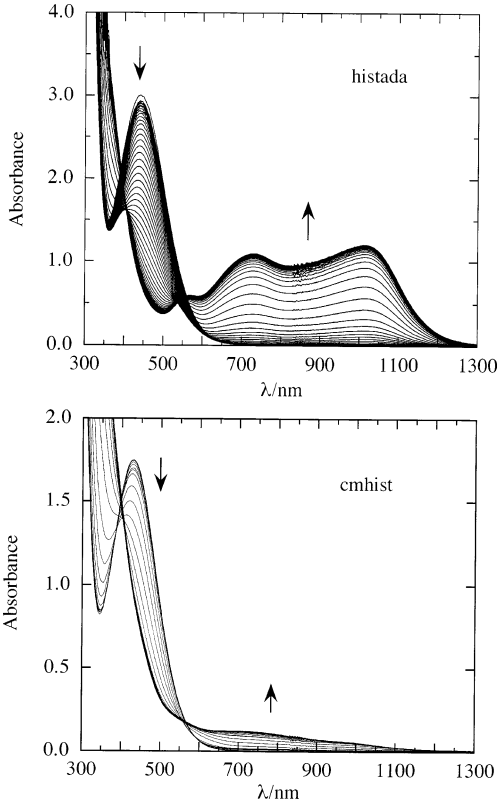

Figure 5. Successive UV−vis absorption spectra observed at 1-h intervals. Upper: $Na[VO(O_2)(histada)]\cdot 3.75H_2O$. Conditions: [complex] = 100 mM, pH 4.50 ($CH_3COONa-HClO_4$), ionic strength = 1.0 M ($NaClO_4$), 1-mm light-path length cell, 30 °C. Lower: $K[VO(O_2)(cmhist)]\cdot H_2O$. Conditions: [complex] = 50 mM, pH 4.51 ($CH_3COONa-HClO_4$), 1-mm light-path length cell, 30 °C. Ionic strength was not adjusted since the solubility of the cmhist complex becomes low in a solution of high ionic strength.

distinction may be due to the difference in the redox potential for the peroxovanadium(V) complexes tuned by the hetero ligands.

EPR Spectra. Since the reduction of diamagnetic vanadium(V) to paramagnetic vanadium(IV) was detected in the described UV−vis spectral measurements, the self-decomposition reaction was followed by the EPR spectrum. The EPR spectral change observed for $[VO(O_2)(histada)]^-$ is shown in Figure 6. The high sensitivity of EPR spectroscopy allows us to detect the EPR signals characteristic to vanadium(IV) species even in an early stage of the self-decomposition process where the reduction of vanadium(V) was not discernible in the UV−vis spectrum. The EPR spectral feature of the solution in which $[VO(O_2)(histada)]^-$ has been completely decomposed is similar to that of the solution containing $K[V^{IV}O(nta)(H_2O)]$ and $K_2[V^{V}O(nta)]$, in which the following equilibrium occurs with a formation constant K of 20 $dm^3\ mol^{-1}$ at 25 °C (I = 1.0 M).[32]

$$[V^{IV}O(nta)(H_2O)]^- + [V^{V}O_2(nta)]^{2-} \rightleftarrows [VO(nta)\text{-}O\text{-}VO(nta)]^{3-} + H_2O$$

The observed spectrum has been explained as a superposition of the 8 hyperfine peaks of the monomeric species and the

(32) Nishizawa, M.; Hirotsu, K.; Ooi, S.; Saito, K. *J. Chem. Soc., Chem. Commun.* **1979**, 707.

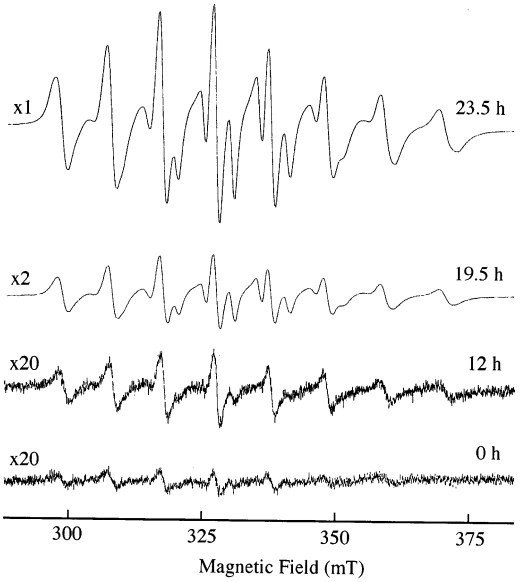

Figure 6. Time-dependent X-band EPR spectra of the decomposition of $Na[VO(O_2)(histada)]\cdot 3.75H_2O$. Solution conditions: [complex] = 100 mM, pH 4.70 ($CH_3COONa-HCl$), ionic strength = 1.0 M (by KCl), 30 °C. EPR conditions: microwave power = 1 mW, microwave frequency = 9.40 GHz, modulation amplitude = 1 G at 100 kHz, receiver gain = 50−1000, sweep time = 8 min.

15 hyperfine peaks of the mixed-valence dimeric species with a delocalized electron. So, the EPR spectrum of the decomposition product of the histada complex confirms the formation of the mixed-valence dinuclear complex. The reaction profile depicted by the EPR intensity is parallel to that depicted by the UV−vis intensity (Supporting Information). The EPR spectrum characteristic of the mixed-valence vanadium complex was also observed for the decomposition product of $[(VO)_2(O_2)_2(dpot)]^{3-}$ (Supporting Information). The EPR spectrum of the completely decomposed cmhist complex was dominated by the 8 hyperfine peaks of the monomeric species though some additional peaks were discernible (Supporting Information). This observation is consistent with the result from the UV−vis measurement described above.

^{1}H and ^{51}V NMR Spectra. The self-decomposition reaction of the dpot complex was followed by ^{1}H and ^{51}V NMR spectrum measurements (Figure 7). In this experiment, buffer solution was not used in order to avoid lowering of the solubility of the dpot complex. As a result, the pD of the solution was raised from 5.19 of the initial solution to 6.73 of the final solution in the decomposition process. The ^{1}H NMR spectrum measured just after dissolving the dpot complex in D_2O contains several weak bands in addition to the bands due to the original complex indicating the instability of the dpot complex. Therefore, it was difficult to assign the observed ^{1}H NMR signals. A probable decomposition product would be the complex in which one of the two peroxo groups dissociated. The easy dissociation of the peroxo group could be rationalized by the unstable coordination of the peroxo group in the dpot complex demonstrated by the large thermal ellipsoids in the ORTEP drawing. Corresponding to the complex ^{1}H NMR spectrum, three signals were observed at −539, −517, and −495 ppm

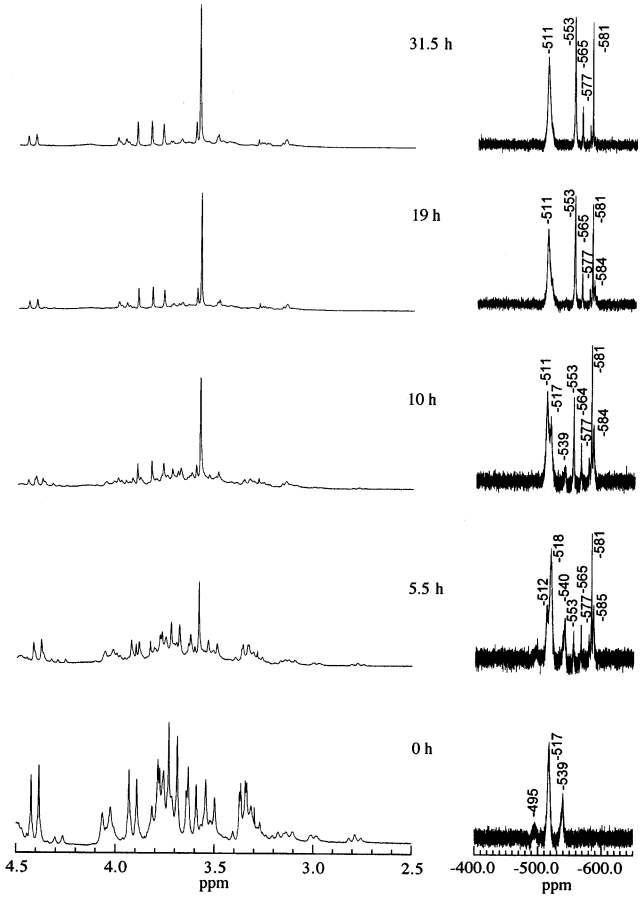

Figure 7. Time-dependent ^{1}H and ^{51}V NMR spectra for the dpot complex. Conditions: [complex] = 30 mM, pD 5.19 (DCl) (buffer solution was not used because of the low solubility of the complex).

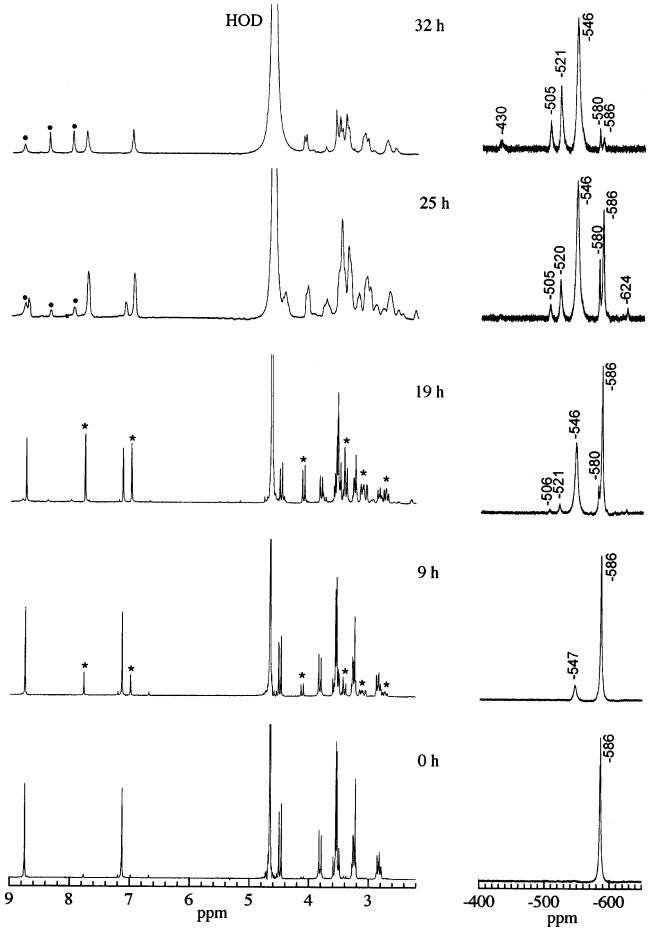

Figure 8. Time-dependent ^{1}H and ^{51}V NMR spectra for the histada complex. Conditions: [complex] = 100 mM, pD 4.91 ($CH_3COONa-DCl$).

in the ^{51}V NMR spectrum. As shown later, an elimination of a coordinating peroxo group in the peroxovanadium(V) complexes results in a lower field shift. Thus, the −539 and −517 ppm signals can be assigned to $[\{VO(O_2)\}_2(dpot)]^{3-}$ and $[(VO_2)\{VO(O_2)\}(dpot)]^{3-}$, respectively. The very weak signal at −495 ppm is due to an unknown species. The final ^{1}H NMR spectrum was relatively simple and similar to the ^{1}H NMR spectrum of the authentic mixed-valence complex, $Cs_4[(V^{V}O)_2(V^{IV}O)_2(\mu\text{-}O)_2(dpot)_2]$ (Supporting Information). $Cs_4[(V^{V}O)_2(V^{IV}O)_2(\mu\text{-}O)_2(dpot)_2]$ was found to be silent in the ^{51}V NMR spectrum. The ^{51}V NMR signal at −511 ppm can, therefore, be assigned to $[(V^{V}O_2)_2(dpot)]^{3-}$. The signals at −553, −565, −577, and −581 ppm are assignable to monomeric and oligomeric species of vanadate,[33] indicating that the dpot ligand in the starting complex was eliminated to some extent in the decomposition process to yield free vanadates. These results as well as the UV−vis results indicate that the vanadium species existing in the final solution are $[(V^{V}O)_2(V^{IV}O)_2(\mu\text{-}O)_2(dpot)_2]$,$^{4-}$ $[(V^{V}O_2)_2(dpot)]^{3-}$, and free vanadates.

Contrary to that of the dpot complex, the ^{1}H NMR spectrum observed just after dissolving $K[VO(O_2)(histada)]$ can be attributed to the intact complex (Figure 8). The signals in the region from 2.6 to 4.6 ppm can be assigned to the methylene protons and those in the region from 7 to 9 ppm to the protons in the imidazole ring. In agreement with the result of ^{1}H NMR study, a single signal was observed at −586 ppm in the ^{51}V NMR spectrum. After 9 h, new signals marked by an asterisk appeared in the ^{1}H NMR spectrum. These signals can be assigned to $[V^{V}O_2(histada)]^{-}$. The corresponding ^{51}V NMR signal appeared at −547 ppm. This assignment was confirmed by the NMR measurement of the solution containing VO_2^{+} and $histada^{2-}$ (Supporting Information). After 19 h, the intensity of these signals increased. At this point, three new signals appeared at −580, −521, and −506 ppm in the ^{51}V NMR spectrum. The signal at −580 ppm would be assigned to tetrameric species of vanadate and the signals at −521 and −506 ppm to decameric species.[33] After 25 h, the further additional ^{1}H NMR signals marked by a solid circle appeared, and all signals became broad, indicating the reduction of V(V) species to paramagnetic V(IV) species. These observations suggest that the coordinated peroxo ligand had dissociated to some extent before the reduction of vanadium(V) was promoted, which is in line with the result obtained from the UV−vis measurements. The broad ^{1}H NMR signals can be mainly attributed to the complexes in equilibrium: $[V^{V}O(histada)-O-V^{IV}O(histada)]^{-} \leftrightarrows [V^{V}O_2(histada)]^{-} + [V^{IV}O(histada)]$.

(33) Rehder, D. Inorganic Considerations on the Function of Vanadium in Biological Systems. In *Metal Ions in Biological Systems: Vanadium and its role in life*; Sigel, H., Sigel, A., Eds.; Marcel Dekker: New York, 1995; Vol. 31.

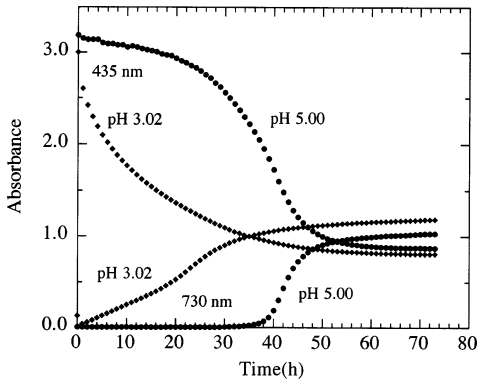

Figure 9. pH dependence of the reaction profiles depicted by the absorbance at 435 and 730 nm for $Na[VO(O_2)(histada)]\cdot 3.75H_2O$. Conditions: [complex] = 100 mM, pH 5.00 and 3.02 ($CH_3COONa-HCl$), ionic strength = 1.0 M (by KCl), 30 °C.

The mixed-valence complex is reasonably considered to be silent in the ^{51}V NMR spectrum. The similar ^{1}H and ^{51}V NMR spectral change was observed for the cmhist complex at pH 5.05 (Supporting Information).

Considering that the species formed in the self-decomposition are relatively simple for the histada complex and that its solubility is high, the following experiments were carried out mainly using the histada complex.

pH Dependence on the Induction Period. In the previous paper, we described that the histada complex is rather stable in a solution of neutral pH but decomposes in an acidic solution.[13] This observation suggests that the length of the induction period would depend on the acidity of the solution. The reaction profile observed at pH 3.02 for the histada complex is compared with that at pH 5.00 in Figure 9. While the induction period was about 38 h long for the solution of pH 5.00, it disappeared for the solution of pH 3.02. This demonstrates that the increase in the acidity of the reaction solution results in the reduction of the induction period. The similar results were obtained for the dpot and cmhist complexes (Supporting Information). Although the induction period was not observed for the solution of pH 3.02, it should be of importance to note that the reaction profile depicted by the absorbance of the intervalence CT band consists of two parts. Namely, the absorbance increases linearly until ca. 18 h and subsequently changes in the similar manner (sigmoid curve) observed at pH 5.00, indicating that the self-decomposition reaction of the histada complex contains at least two processes.

The protonated complex has been isolated from the acidified solution (pH 3.5) of $K[VO(O_2)(cmhist)]$.[13] The protonation has been considered to occur at the carboxylato group, and the alternative formulation, $[VO(O_2)(Hcmhist)]$ or $[VO(O_2)(Hcmhist)(H_2O)]$, has been proposed for the protonated complex. If the dimerization process is a key step in the self-decomposition reaction as suggested by Bonchio et al.,[6] a free coordination site should be available for the dimerization of the histada and cmhist complexes. Then, the promotion of the self-decomposition reaction by proton can be regarded as a result producing a free coordination site by protonation of the carboxylato group. According to this view, the protonated complex would be reasonably formulated as $[VO(O_2)(HL)(H_2O)]$, where one carboxylato group is uncoordinated due to the protonation.

It has been known that $[VO(O_2)(nta)]^{2-}$ is very stable even in an acidic solution and does not show any tendency to form a dimeric complex in solution. The coordination environment of the nta complex is rigid compared to the histada and cmhist complexes, which is evidenced by the ^{1}H and ^{51}V NMR measurements (Supporting Information). In fact, the ^{1}H NMR spectrum of the nta complex in a fairly acidic solution (pH 2.52) is the same as that observed at neutral pH. The corresponding ^{51}V NMR spectrum shows a single peak at −555 ppm. These observations imply that a free coordination site necessary for dimerization cannot be available for the nta complex. On the other hand, the cmhist (pH 3.51) and histada (pH 2.25) complexes exhibited additional signals in the ^{1}H NMR spectrum. Namely, in the ^{1}H resonance region of the imidazole ring of the cmhist complex, the additional signals assignable to NC*H*C appeared at 7.25 and 7.29 ppm besides the signal of the intact complex at 7.02 ppm. The signals due to NC*H*N overlap with that of the intact complex at 8.50 ppm. Corresponding to the ^{1}H NMR spectrum, the additional signals appeared at −603 and −594 ppm besides the original peak (−621 ppm). These additional signals cannot be attributed to the complex without the peroxo group, $[VO_2(cmhist)]^-$, which exhibits a ^{51}V NMR signal at −546 ppm. The ^{1}H NMR signals of the imidazole group of $[VO_2(cmhist)]^-$ (7.00 and 7.86 ppm) were not also observed. Thus, the additional signals can be assigned to the resonances of peroxovanadium(V) complexes with the cmhist ligand of which the coordination mode was modified by protonation. The modification in the coordination mode would be a tridentate coordination of the cmhist ligand due to a protonation of the carboxylato group leaving a free coordination site, which results in the formation of $[VO(O_2)(HL)(H_2O)]$ as shown above. The observation of two sets of the additional signals suggests that two geometrical isomers may exist in the solution. For the histada complex, the additional NC*H*C signals appeared at 7.06 and 7.22 ppm besides the signal of the intact complex at 7.03 ppm. The additional NC*H*N signals appeared at 8.39 and 8.50 ppm besides the signal of the intact complex at 8.65 ppm. The very weak signals assignable to $[VO_2(histada)]^-$ were also observed at 6.90 and 7.66 ppm. In the ^{51}V NMR spectrum, the additional signals were observed at −546, −553, −567 (very weak) ppm besides the original peak (−587 ppm). The additional signals at −553 and −567 ppm cannot be attributed to $[VO_2(histada)]^-$ (−546 ppm). Thus, these signals can be attributed to $[VO(O_2)(Hhistada)(H_2O)]$ as for the cmhist complex. (Although the signal at −546 ppm is in the same position as $[VO_2(histada)]^-$, its intensity is higher than that expected from the corresponding ^{1}H NMR signals, suggesting a superposition with a signal due to isomeric species of $[VO(O_2)(Hhistada)(H_2O)]$.) In conclusion, it is reasonably considered that the histada and cmhist ligands coordinate in a tridentate fashion by protonation in acidic solution, leaving a free coordination site on the vanadium center.

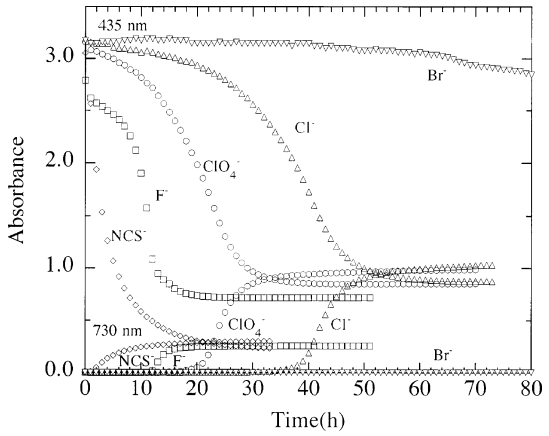

Figure 10. Variation of the reaction profiles depending on the coexisting anion for the histada complex. Conditions: [complex] = 100 mM, 30 °C; Br^- system, pH 5.00 ($CH_3COONa-HBr$), ionic strength = 1.0 M (by KBr); Cl^- system, pH 5.00 ($CH_3COONa-HCl$), ionic strength 1.0 M (by KCl); ClO_4^- system, pH 5.03 ($CH_3COONa-HClO_4$); F^- system, pH 6.68, ionic strength = 1.0 M (by KF); NCS^- system, pH 4.95 ($CH_3COONa-HCl$), [NaSCN] = 690 mM.

Although we cannot conclude necessarily because the redox potential of the monomeric complex affects the reduction of vanadium(V), it is anticipated that the monomeric peroxovanadium(V) complexes that can form dimers in an acidic solution undergo the decomposition accompanying the reduction of vanadium(V) to vanadium(IV) more readily.

Dependence on the Coexisting Anions. The self-decomposition profiles of the histada complex were compared for the solutions containing F^-, Cl^-, Br^-, ClO_4^-, and NCS^- anions in order to examine the effect of the coexisting anion on the self-decomposition process. As mentioned earlier, perchlorate can be considered to be innocent in the self-decomposition process. The UV−vis measurement of the fluoride system was performed at pH 6.68 to avoid the erosion of the quartz cell due to hydrogen fluoride. The experiments using other coexisting anions were done around pH 5. The comparison of the anion dependence on the reaction profile among the halogen species should be of importance since the histada complex mimics the active site of the vanadium-dependent haloperoxidases (VHPO). A clear difference can be noticed among the reaction profiles of the histada complex as shown in Figure 10. The induction period of the chloride system is longer than that of the perchlorate system, suggesting the chloride anion suppresses the self-decomposition of the histada complex to some extent. The inhibition of the self-decomposition is distinct for the bromide system. Vanadium(V) has scarcely reduced until at least 100 h in this system while the intensity of the peroxo CT band slightly decreased. This difference in the reaction profiles would be explained on the basis of the fact that bromide is more easily oxidized than chloride. Thus, in the bromide system, bromide would be oxidized by the peroxo group (or other active oxygen species produced) in preference to the reduction of vanadium(V) induced by the peroxo group. Namely, it can be considered that bromide inhibits an accumulation of radical species necessary for an initiation of the full radical chain reaction. An alternative explanation could be that bromide coordination would stabilize the peroxovanadium(V) complex, though a mechanism is not clear.

Contrary to the bromide system, the induction period of the fluoride system is shorter than that of the perchlorate system, regardless of the pH of the solution of the fluoride system being higher than that of the perchlorate system. Another characteristic of the fluoride system is that, despite the peroxo CT band disappearing quickly, the increase in the intervalence CT band is to a far less extent compared to the Cl^- and ClO_4^- systems. This observation can be explained as follows. Since fluoride anion has a higher ligand-field strength than chloride and bromide, it would substitute the peroxo ligand to yield $[VO_2(histda)]^-$, which results in the rapid disappearance of the peroxo CT band. This assumption is supported by NMR measurements (Supporting Information). The ^{51}V NMR spectrum observed after 30 h shows a signal due to $[VO_2(histda)]^-$ at −545 ppm. In addition to this signal, two signals were observed at −579 and −587 ppm. The former signal can be assigned to a tetramer of vanadate and the latter to a pentamer,[33] suggesting that the elimination of the histada ligand also occurred.

In order to confirm this assumption, the self-decomposition reaction of the solution containing thiocyanate anion, of which the ligand-field strength is stronger than those of halides, was examined. The reaction profile is included in Figure 10. The peroxo CT band rapidly disappears while the reduction of vanadium(V) is suppressed in a similar manner as the fluoride system. Walker and Butler have shown that thiocyanate is preferentially oxidized by vanadium bromoperoxidase over bromide.[34] In our present case, however, a substitution of the peroxo group by thiocyanate would be responsible for the change in the reaction profile since the reaction profile of the thiocyanate system is similar to that of the fluoride system and different from the bromide system. This assumption was substantiated by the ^1H and ^{51}V NMR spectra of the $[VO(O_2)(histada)]^-/NCS^-$ systems, in which the ^1H NMR signals and ^{51}V NMR signal (−546 ppm) due to $[VO_2(histada)]^-$ were observed (Supporting Information). Then, it can be reasonably assumed that elimination of the peroxo group from the coordination sphere suppresses the reduction of vanadium(V); in other words, the reduction of vanadium(V) is induced mainly by the coordinated peroxo group.

The anion dependence on the reaction profile for the dpot complex shows a similar tendency to the histada complex in general, but some differences were also discerned (Supporting Information). The difference in the reaction profiles between perchlorate and chloride systems is small, and the amount of the mixed-valence complex is reduced for the perchlorate system. Although the histada complex negligibly decomposed in the presence of bromide, the dpot complex decomposed slowly. The effect induced by F^- is pronounced compared to the histada complex but that by NCS^- is small. These differences may be due to the dimeric structure and/or the complex composition of the initial solution of the dpot

(34) Walker, J. V.; Butler, A. *Inorg. Chim. Acta* **1996**, *243*, 201.

Scheme 1. Production of Radical Species by Reaction of $V(IV)O^{2+}$ and $V(V)O_2^+$ with H_2O_2

$$V(IV)O^{2+} + H_2O_2 \longrightarrow V(V)O_2^+ + H^+ + HO\bullet \quad (1)$$

$$V(V)O_2^+ + H_2O_2 \longrightarrow V(V)O(O_2)^+ + H_2O \quad (2)$$

$$V(V)O(O_2)^+ + H_2O_2 \longrightarrow V(V)O_3^\bullet + HOO\bullet + H^+ \quad (3)$$

$$V(V)O(O_2)^+ + H_2O_2 \longrightarrow V(IV)O^{2+} + O_2 + HO^- + HO\bullet \quad (4)$$

complex. The anion dependence on the reaction profile for the cmhist complex was not able to be examined because of its low solubility in aqueous solution containing inorganic salts.

Effects Induced by an Addition of Vanadate(V) and Vanadyl(IV) Ions. According to the literature,[6] the induction period of the self-decomposition reaction of peroxovanadium(V) species is the period until the full radical chain reaction is initiated. The reactions between peroxide and $V^VO_2^+$ or $V^{IV}O^{2+}$ produce radical species by the known reactions shown in Scheme 1. We have therefore examined the effects induced by the addition of 1/100 equiv of vanadate(V) or vanadyl(IV) ions on the self-decomposition reaction of the histada complex. Since free peroxide is available through dissociation from the peroxo histada complex, the extra peroxide was not added to the reaction solution. The observed reaction profiles are shown in Figure 11A. As expected, the addition of a small amount of vanadate(V) and vanadyl(IV) ions significantly reduces the induction period. Vanadyl(IV) ion has a larger influence than vanadate(V) on the reduction of the induction period. Similar phenomena were observed for the dpot and cmhist complexes (Supporting Information).

Effects Induced by the Addition of Radical Scavengers. It has been shown that the length of the induction period in the self-decomposition reaction of the peroxovanadium(V) species can be extended by addition of radical scavenger DTBC (di-*tert*-butyl-*p*-cresol).[6] We thus examined the effect of several radical scavengers (Scheme 2) on the length of the induction period in the self-decomposition reaction of the histada complex. TBPC (2-*tert*-butyl-*p*-cresol) was used instead of DTBC since DTBC is scarcely soluble in water. The system containing trolox was also examined. Trolox is a water-soluble analogue of vitamin E known to scavenge hydroxyl radical and is commonly used in biological experiments. The reaction profiles observed for the histada complex are shown in Figure 11B. The length of the induction period is appreciably extended by the addition of 1/100 equiv of TBPC as expected. In contrast, addition of trolox reduced the length of the induction period remarkably. It should be noted that trolox accelerates the disappearance of the peroxo CT band as F^- and NCS^- but does not suppress the reduction of vanadium(V). Thus, it can be considered that trolox would act as an initiator or a promoter of the full radical chain reaction though the detailed mechanism is unknown at present.[35]

As these spectroscopic studies suggest that active oxygen species are generated in the self-decomposition reaction of the peroxovanadium(V) complexes, we have tried to detect the active oxygen species. The oxidizing ability of the active

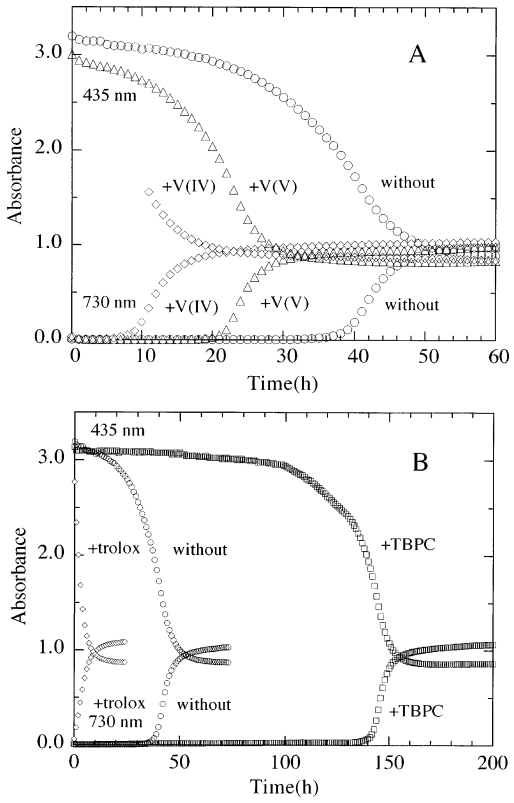

Figure 11. Variation of the reaction profiles induced by an addition of V(IV) and V(V) species (A), and radical scavengers (B) for the histada complex. Conditions: [complex] = 100 mM, ionic strength = 1.0 M (by KCl), buffer $CH_3COONa-HCl$, 30 °C; V(IV) system, pH 5.00, $[VOSO_4]$ = 1 mM; V(V) system, pH 5.01, $[Na_3VO_4]$ = 1 mM; TBPC system, pH 5.03, [TBPC] = 1 mM; trolox system, pH 4.94, [trolox] = 10 mM. Early time data of the 435-nm absorbance for the V(IV) containing system could not be obtained because the absorbance at early times went over the measurable range of the spectrometer by addition of vanadyl(IV) sulfate.

Scheme 2. Radical Scavengers

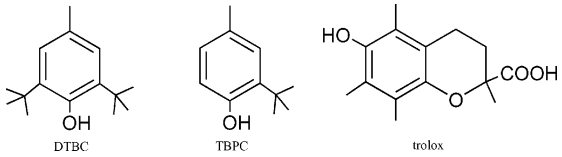

oxygen species generated in the self-decomposition process is also evaluated.

Detection of Active Oxygen Species. In the self-decomposition process of the peroxovanadium(V) complexes, vanadium(V) was partly reduced as shown above. One probable route for the formation of vanadium(IV) species would be one electron transfer from the peroxo group to vanadium(V). If the above direct reduction of vanadium(V) by the peroxo group would occur, superoxide anion would be produced in the self-decomposition process. Superoxide anion can also be produced according to reaction 3 in Scheme 1. Therefore, we attempted to detect superoxide anion in the self-decomposition of the cmhist complex. In the method

(35) One reviewer suggested that the difference between Trolox and TBPC is because Trolox has a lower oxidation potential than TBPC and is much more easily oxidized by vanadates. Another suggestion is that the chroman moiety of Trolox with hydrogen peroxide would give several radical side reactions that might be responsible for the observed shortening of the induction period.

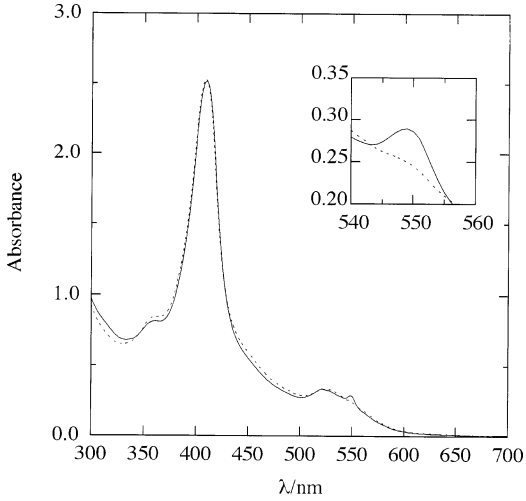

Figure 12. Absorption spectra of the solution containing cytochrome *c* (30 mM) and the cmhist complex (1 mM): dotted line, reaction time = 0; solid line, reaction time = 15 min.

utilizing the reduction of cytochrome *c*,[22] the absorption spectral change was observed as shown in Figure 12. The 550-nm band observed after 15 min can be assigned to the reduced form of cytochrome *c*. It was estimated from the intensity of the 550 nm band that ca. 2.9% of superoxide anion was produced on the basis of the decomposition amount of the cmhist complex (see Experimental Section for details). This method was not useful for the dpot and histada complexes since the absorption spectral change was not large enough to permit exact evaluation. So, we tried the WST-1 method to detect superoxide anion.

In the WST-1 assay, the relative amounts of the superoxide anion produced in the self-decomposition process of the dpot, histada, and cmhist complexes were calculated to be ca. 3.8%, ca. 1.8%, and ca. 6.6%, respectively, on the basis of the decomposition amount of each complex (see Experimental Section for details). Although some discrepancy exists in the amount of superoxide anion for the two independent assays for the cmhist complex, the detected amounts of superoxide anion produced in the self-decomposition process of the peroxovanadium(V) complexes were quite small. These results indicate that the direct reduction of vanadium(V) by the peroxo group and reaction 3 in Scheme 2 are not predominant reactions and/or the superoxide anion produced in the self-decomposition process was transferred to another reactive oxygen species (ROS). Thus, we attempted to detect other ROS.

By using an EPR spin trapping technique, we successfully detected the specific EPR spectrum of the DMPO−OH adduct accompanying the decomposition of the dpot, histada, and cmhist complexes (Figure 13).[25] DMPO also reacts with superoxide anion to form a DMPO−OOH adduct.[25b,36] However, we could not detect the EPR spectrum specific to the DMPO−OOH adduct, suggesting that the total amount of superoxide anion formed in the self-decomposition of the peroxovanadium(V) complexes is small. This is consistent

(36) Kohno, M.; Yamada, M.; Mitsuta, K.; Mizuta, Y.; Yoshikawa, T. *Bull. Chem. Soc. Jpn.* **1991**, *24*, 1285.

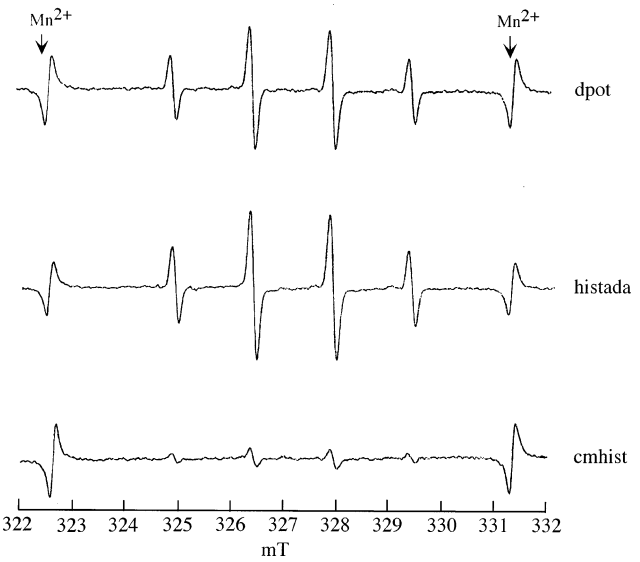

Figure 13. EPR spectrum of the solutions containing the dpot complex (100 mM), the histada complex (75 mM), and the cmhist complex (75 mM) and DMPO (610 mM) at pH 7.4 recorded after 15 min from mixing.

Scheme 3. Probable Reactions via Dimeric Intermediate to Yield the Mixed-Valence Dinuclear Vanadium Complex

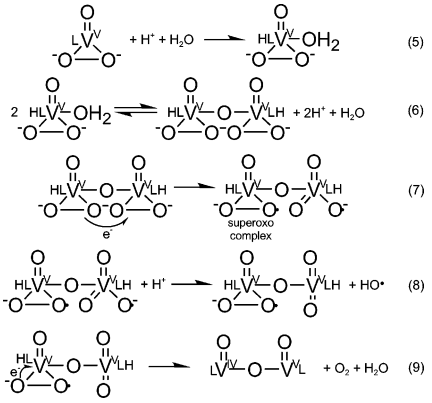

with the results obtained in the superoxide assay already mentioned. Thus, it can be concluded that hydroxyl radical, but not superoxide anion, is the major product in the self-decomposition process of the peroxovanadium(V) complexes.

Probable Reactions in the Self-Decomposition Process. We propose here the probable reactions to yield the V(IV)−V(V) mixed-valence dinuclear complexes based on the information obtained in this study and by referring the mechanism proposed by Bonchio et al.[6] Successive reactions via a dimeric intermediate are shown in Scheme 3. First, a free coordination site is produced by the protonation of the chelate (reaction 5). The protonated complex has been isolated for the cmhist complex.[13] In the next step (reaction 6), two monomeric complexes associate to give a dimeric intermediate proposed in the reference.[6] Of course, these two steps are not necessary for the dpot complex. Then, one-electron transfer occurs intramolecularly from a peroxo group in a monomeric moiety to a peroxo group in another monomeric moiety (reaction 7). This process has been proposed on the basis of the kinetic study.[6] A monomeric moiety donating one electron changes a superoxovanadium(V) complex. A superoxovanadium(V) complex has been

Scheme 4. Other Probable Reactions

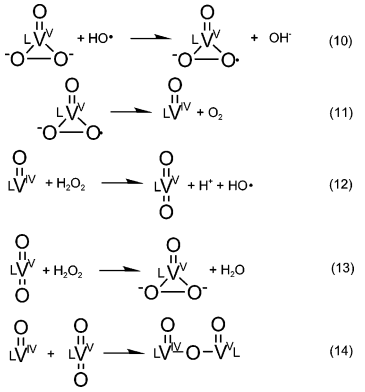

established by EPR spectroscopy.[37] An unstable superoxovanadium(V) complex undergoes one-electron transfer intramolecularly from a superoxo ligand to a vanadium(V) center, resulting in the formation of vanadium(IV) species and molecular oxygen (reaction 9).[38] The superoxide anion detected in this study could be formed by dissociation from the superoxo complex. On the other hand, in a monomeric moiety accepting one electron, the peroxo bond cleaves, resulting in a formation of hydroxyl radical (reactions 7 and 8). A hydroxyl radical was detected in the self-decomposition process of the peroxovanadium(V) complexes as shown in the previous section. Although there is no evidence that the dimeric unit is maintained through the reactions for the cmhist and histada systems, reactions 7−9 should occur within the dimeric unit at least in the dpot complex since two vanadium centers are tightly connected by a dinucleating ligand.

Although the reactions in Scheme 3 are likely to occur, a more complex mechanism would actually operate in the self-decomposition process. We postulate the reactions shown in Scheme 4, in which a monomeric complex (or a monomeric moiety in the case of the dpot complex) operates. These reactions have been established[6] and are consistent with the fact that the radical chain reaction initiates after dissociation of the peroxo coordination proceeds to some extent as evidenced by the UV−vis and ^{1}H and ^{51}V NMR studies. The formation of the mixed-valence dinuclear complex would act as a termination reaction in this case.

Although it cannot be concluded at present which mechanism (Scheme 3 or 4) operates primarily in the self-decomposition process of the peroxovanadium(V) complexes, it is presumed that the reactions in Scheme 3 act as initiation reactions for the radical chain reaction by producing hydroxyl radical.

Oxidizing Ability. It has been proposed that peroxovanadium(V) complexes activate tyrosine kynase by inhibition phosphotyrosine phosphatase (PTPase) in their insulin mimetic action.[10] Since the α-subunit of the insulin recepter contains cysteine-rich species, it has been suggested that the oxidative coupling of cysteine residues would explain a part of the insulin mimetic effect of the peroxovanadium(V) complexes.[11]

(37) Brooks, H. B.; Sicilio, F. *Inorg. Chem.* **1971**, *10*, 2530.
(38) Thompson, R. C. *Inorg. Chem.* **1982**, *21*, 859.

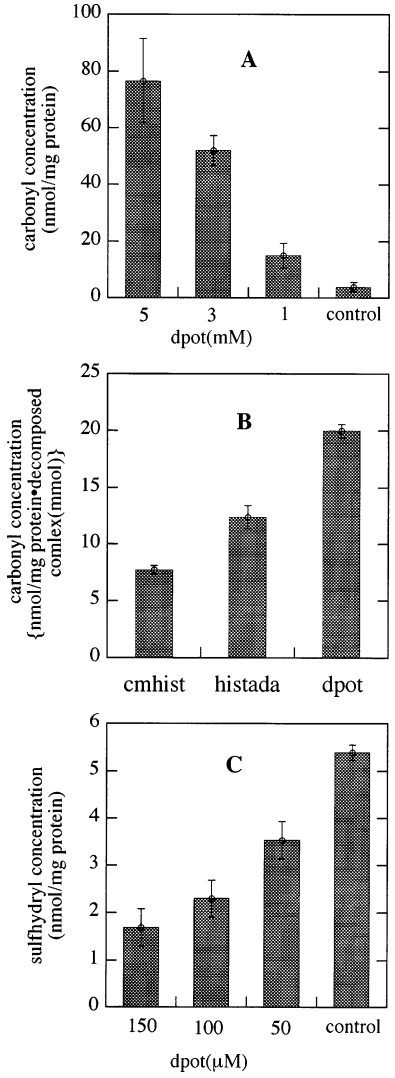

Figure 14. (A) Carbonyl concentration in BSA oxidized by the dpot complex. (B) Comparison of the carbonyl concentrations in BSA oxidized by the cmhist, histada, and dpot complexes. (C) Sulfhydryl concentration in BSA oxidized by the dpot complex.

Since it has been established that reactive oxygen species are produced in the self-decomposition process of the peroxovanadium(V) complexes, we examined the oxidizing ability of the dpot, histada, and cmhist complexes toward a protein BSA as a measure of the oxidative ability of the peroxovanadium(V) complexes. In the protein carbonyl assay, the carbonyl concentration of BSA increased significantly against a control sample with 5 and 3 mM of the dpot complex (Figure 14A). By comparing the oxidizing ability of the peroxovanadium(V) complexes toward BSA, we found that the dpot complex has the highest oxidizing ability toward BSA among three peroxovanadium(V) complexes (Figure 14B). Previously, we have compared the oxidizing abilities of peroxynitrite, hydroxyl radical (Fenton reaction, NP-III (*N*,*N*′-bis(2-hydroperoxy-2-methoxyethyl)-1,4,5,8-naphthalenetetracarboxylic diimide)), and hypochlorite toward bovine serum albumin (BSA).[39] The hydroxyl radical generated, especially by NP-III, increased markedly the amount of

(39) Yasui, F.; Matsugo, S. *ITE Lett.* **2001**, *2*, 537.

protein carbonyl formation, whereas the nonradical oxidants such as peroxynitrite and hypochlorite did not. On the other hand, it was proven by an ESR method that the peroxovanadium(V) complexes used in this experiment generate hydroxyl radical in the self-decomposition process, suggesting that the peroxovanadium(V) complexes have an excellent oxidizing ability as well as Fenton reaction and NP-III. When the amounts of protein carbonyl formation by these three oxidants were compared, the amounts formed by the peroxovanadium(V) complexes were smaller than those from Fenton reaction and NP-III. This result is reflecting the difference in the amount of hydroxyl radical generation between Fenton reaction, NP-III, and peroxovanadium(V) complexes. In the protein sulfhydryl assay, the sulfhydryl concentration of BSA decreased significantly against a control sample with increasing concentration of the dpot complex (Figure 14C). The sulfhydryl residues in BSA were oxidized ca. 35% and 70% by 50 and 150 μM dpot complex, respectively. However, the degree of the sulfhydryl oxidation by hydroxyl radical was weaker compared with peroxynitrite. As for oxidation of the protein by the present complexes, protein carbonyl formation will take place preferentially. Considering that protein carbonyl formation occurs effectively by hydroxyl radical while the degree of the sulfhydryl oxidation by hydroxyl radical is small compared to nonradical oxidants such as peroxynitrile, the peroxovanadium(V) complexes used in the present study may act as a nonradical oxidant in the sulfhydryl oxidation. Regarding the reactive oxygen species generated from vanadium, Zhang et al. reported that those generated from vanadate induce the cell growth arrest at the G_2/M phase.[40] Thus, this strong oxidizing ability of the peroxovanadium(V) complexes toward biomolecules such as protein is one of various functions of peroxovanadium(V) complexes in vivo.

(40) Zhang, Z.; Leonard, S. S.; Huang, C.; Vallyathan V.; Castranova, V.; Shi, X. *Free Radical Biol. Med.* **2003**, *34*, 1333.

Supporting Information Available: NMR, EPR, and UV−vis spectra, decomposition profiles, and X-ray crystallographic information including final atomic coordinates, anisotropic thermal parameters, and full bond lengths and angles in CIF format. This material is available free of charge via the Internet at http://pubs.acs.org.

IC030292F